Primer sequences

Mouse adiponectin receptor 1 and adiponectin receptor 2: 5'-ACGTTGGAGAGTCATCCCGTAT-3', mouse adiponectin receptor 1 (forward); 5'-CTCTGTGTGGATGCGGAAGAT-3', mouse adiponectin receptor 1 (reverse); 5'-GCCCAGCTTAGAGACACCTG-3', mouse adiponectin receptor 2 (forward); 5'-GCCTTCCCACACCTTACAAA-3', mouse adiponectin receptor 2 (reverse). PCR primers used to genotype adiponectin wildtype, heterozygous, and knockout mice: 5'-TGGATGCTGCCATGTTCCCAT-3', wildtype adiponectin (forward); 5'-CTTGTGTCTGTGTCTAGGCCTT-3', wildtype adiponectin (reverse); 5'-CTCCAGACTGCCTTGGGA-3', mutant adiponectin (reverse).

Immunoblotting

To detect the different isoforms of adiponectin in mouse serum or bone marrow, samples were electrophoresed through non-denaturing and non-reducing 4-12% SDS gels. Protein was transferred to nitrocellulose membranes and probed with rabbit anti-mouse adiponectin (ABCAM, Cambridge, MA) at a 1:2,000 dilution. Secondary antibody was used at a 1:5,000 dilution and signal was detected using ECL reagents (Amersham, U.K.). Densitometry was performed using ImageJ software (NIH).

Total cell lysates for western blot analysis were prepared by lysing cell pellets in RIPA buffer containing 1 mM EDTA. Protein lysates were separated by SDS-PAGE, transferred to polyvinylidene difluoride (PVDF) membranes and then blocked in TBS plus 5% BSA and 0.1% TWEEN for 1hour, before incubating with anti-phosphorylated AMPK (Cell Signaling), anti-total AMPK (Cell Signaling), anti-

phosphorylated p38 (Santa Cruz), anti-total p38 (Santa Cruz), anti-cleaved caspase 3 (Cell Signaling) or anti-cleaved PARP-1 (Cell Signaling) or anti-β-actin at 4^{o}C overnight. Antigen-antibody complexes were detected using secondary antibodies conjugated to HRP and visualized by enhanced chemiluminescence ECL (Amersham).

Bone histomorphometric analysis and immunohistochemistry

Histomorphometric analysis was performed to quantify bone volume, osteoclast and osteoblast number and surface, trabecular number and trabecular spacing. Tibia and femur were formalin-fixed, decalcified in 14% EDTA, paraffin-embedded, sectioned along the mid-sagittal plane in 4-μm-thick sections. Sections were stained with haematoxylin and eosin and for tartrate-resistant acid phosphatase (TRAP) activity to stain osteoclasts. For visualization of calcein green labeling, spines were fixed in 70% ethanol and embedded in methylmethacrylate without prior decalcification. 6uM thick sections were cut and viewed unstained by epi-fluorescence microscopy. Three non-consecutive sections were evaluated using Osteomeasure histomorphometry software as previously described (Edwards et al., 2008).

Tibia sections adjacent to those used to assess bone disease were immunohistochemically stained for TUNEL (AP kit, Roche) for quantification of apoptotic myeloma cells and ki-75 and p-histone H3 to measure proliferating myeloma cells. Detailed methods are described in Supplemental Procedures. For antigen retrieval, slides were then incubated in 100mM citrate buffer for 1-2 minutes in microwave. After washes, sections were blocked in solution containing 3% BSA and 20% FCS for TUNEL or in 10% normal goat serum for histone H3, for 1 hour at

room temperature. Histone H3 antibody was diluted 1:500 in blocking solution and incubated overnight at 4^{o}C. Following washes, histone H3 sections were incubated at room temperature for 1 hour in species-specific biotinylated secondary antibody diluted 1:500 in appropriate blocking solution. For Ki-67, sections were incubated with a 1:200 dilution of a polyclonal antibody to Ki67 (Abcam Inc. Cambridge, MA). For TUNEL stained sections, the manufacture's protocol was followed accordingly. TUNEL reaction mixture was prepared fresh and sections incubated in mixture for 1 hour at 37^{o}C. Slides were washed following incubation and then incubated with Converter-AP for 30 minutes at 37^{o}C. The substrate solution was applied to TUNEL sections for 10 minutes at room temperature. Following staining procedures, slides were aqueously mounted in media (Biomeda Corp). Apoptotic or proliferating myeloma cells were scored blind to generate a proliferation or apoptotic index using MetaMorph (Molecular devices) computer software. 5 fields were assessed per tumor at x40 magnification.

MicroCT analysis

Tibiae were fixed in formalin, and each bone was scanned at an isotropic voxel size of 12μm using a microCT40 (SCANCO Medical, Bassersdorf, Switzerland). In analyzing the reconstructed images, contours were drawn within the cortices around the metaphyses, such that the total volume (TV) included only trabecular bone at 0.2mm below the growth plate and extending 0.12mm. Bone volume (BV) included all bone tissue that had a material density greater than 438.7 mgHA/cm^{3}, thereby giving a measure of BV/TV. The same threshold setting for bone tissue was used for all samples. For analysis of cortical bone lesions, the region of interest was the entire metaphysis including the cortices and extending 0.25mm from the growth plate. The

cross-sectional images of this region were exported in tiff format and imported into AMIRA three dimensional graphics software. Again using a consistent threshold, AMIRA generated three dimensional renderings of the metaphyses. Rotating the virtual bone through 360^{o}, the numbers of osteolytic lesions were counted which completely penetrated the cortical bone and were greater than 100μm in diameter.

Table S1. Patient characteristics and biochemical data

	All			Male			Female		
	Control	MGUS with progression	MGUS no progression	Control	MGUS with progression	MGUS no progression	Control	MGUS with progression	MGUS no progression
Age (years)	67.0 ± 1.4	66.7 ± 1.8	67.5 ± 2.2	68.0 ± 1.0	68.9 ± 1.4	67.9 ± 1.6	65.4 ± 1.8	66.3 ± 3.3	64.4 ± 2.2
BMI (kg/m^2)	28.0 ± 0.8	29.0 ± 1.1	27.6 ± 1.1	29.0 ± 0.6	29.3 ± 0.9	29.0 ± 1.1	27.2 ± 1.0	28.8 ± 1.4	27.4 ± 0.8
Glucose (mg/dL)	85.0 ± 4.1	77.5 ± 2.4	79.7 ± 3.5	86.0 ± 1.9	79.5 ± 2.0	80.1 ± 3.6	82.6 ± 5.9	75.4 ± 2.8	78.9 ± 3.6
Testosterone (ng/ml)	10.26 ± 1.1	12.3 ± 0.1	11.6 ± 1.2	12.6 ± 1.0	14.7 ± 1.4	14.0 ± 1.0	4.7 ± 0.7	5.38 ± 0.26	6.09 ± 0.13

Data are expressed as mean ± SEM

Table S2. Bone parameters of Rag2-/-Adipo-/- and Rag2-/- Adipo+/+ mice. MicroCT and histomorphometric analysis of wild-type and adiponectin deficient mice.

	$Rag2^{-/-}/Adipo^{+/+}$	$Rag2^{-/-}Adipo^{-/-}$	p-value
% BV/TV	5.48 ± 0.67	3.82 ± 0.75	0.130
OB.S/B/S (mm^2/mm^3)	15.6 ± 1.23	16.4 ± 1.96	0.759
OC.S/B.S (mm^2/mm_3)	15.3 ± 1.27	17.5 ± 1.9	0.384
Tb.N. (1/mm)	4.71 ± 0.35	3.95 ± 0.5	0.251
Tb.Th (mm)	0.04 ± 0.003	0.04 ± 0.001	0.189
Tb.Sp. (mm)	0.22 ± 0.02	0.27 ± 0.05	0.323

trabecular bone volume (%BV/TV), osteoblast surface (OB.S/BS) and osteoclast surface to bone surface (OC.S./BS), trabecular number (Tb.N.), trabecular thickness (Tb.Th.), and trabecular spacing (Tb.Sp.). Data are expressed as mean ± SEM, n=5.

Figure S1. High molecular weight adiponectin serum concentrations measured by ELISA in myeloma non-permissive C57Bl6 and permissive C57Bl/KaLwRij mice. Data are represented as mean ± SEM, n=8.

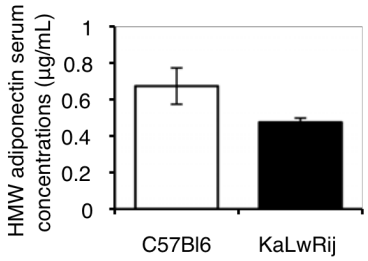

Figure S2. Western blot analysis showing lack of adiponectin expression (total and different isoforms) in serum of RAG-2$^{-/-}$Adipo$^{-/-}$ mice in comparison to wild-type mice. Each lane represents serum from one mouse.